Analysis note 42 : Proton and Anti–proton Analysis.

December 13, 2002

by

Peter Christiansen, NBI, pchristi@nbi.dk

1 Introduction

The purpose of the note is to give an overview of my analysis. There are probably a lot of spelling errors since we have a problem with ispell and emacs here.

2 Data Selection

For all the data presented, a centrality cut selecting the top 10% events was applied. For the MRS the vertex range from -15 to +15 have been used and for the FFS and FS the vertex range from -20 to +20 have been used.
I have not used the ZDC vertex or the cluster vertex.

2.1 MRS Selection

The MRS PID was done based on cuts in m^2 calculated from the TOFW TOF and the D5 momentum p. Event though there is a momentum dependence I used a constant cut which I estimated was at least 3 sigmas at $p \sim 3$ GeV so no corrections had to be applied for the data selection. It would be interesting to understand the momentum dependence better and push the PID to 4 GeV in some limited window and see if we can reproduce the STAR $\bar{p}/p$ results.
An important cut for the protons is the vertex cut. First all tracks are projected back to the beam line and compared to the interaction point determined by the BB counters. The residuals are fitted with gaussians to obtain the means and sigmas (μ_Y, μ_Z, σ_Y, and σ_Z). The resolution in y is determined by the TPM1 track and the resolution in z is dominated by the BB resolution. Typical values are $\sigma_Y \approx 0.4$ cm and $\sigma_Z \approx 0.8$ cm. The distribution has long tails that are believed to primarily come from decays and knocked out particles. The effect of the vertex cut is shown in Fig 1. By comparing the effect on anti–protons and protons it is clear that the cut primarily removes protons produced in material (beam pipe etc.) with $p_T < 1.3$ GeV.
When the tracks from TPM1 and TPM2 are matched in the D5 magnet the tracks are required to propagate through the D5 magnet without getting closer than 1 cm to the magnet (fiducial cut). The effect of this cut is shown in Fig. 2. Since the height of the D5 magnet is ~ 10 cm the effect of cutting out 2 cm reduces the data by ~ 20 %. It would be good if we could use a smaller fiducial cut, but the quality of the match–up in the vertical (y) direction currently does not allow this.
The cuts used in the MRS analysis is summarised in Table 1. The protons selected in the 90° degree 1000B setting is shown in Fig. 3. It is clear that the background is negligible here. When we go forward the resolution and the background problems gets worse, see Figure 4.

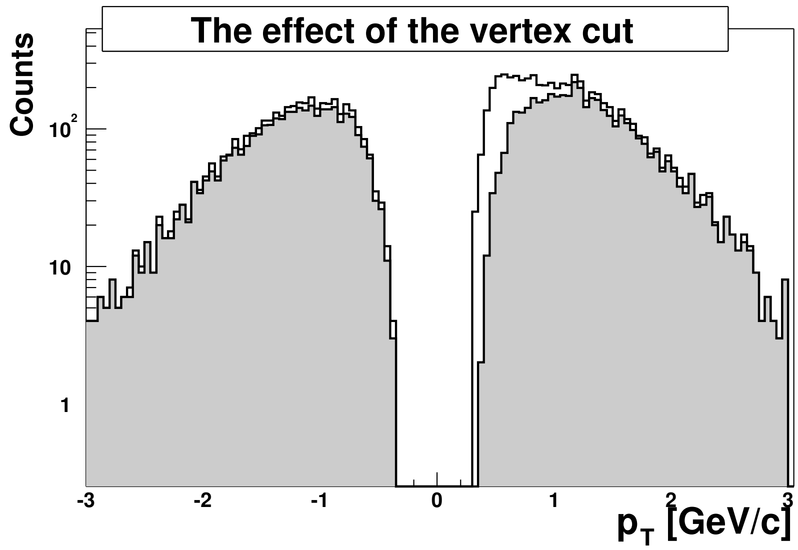

Figure 1: The effect of the vertex cut on protons (positive p_T) and anti–protons (negative p_T). The effect on the protons is much larger than on the anti-protons suggesting that primarily background is removed.

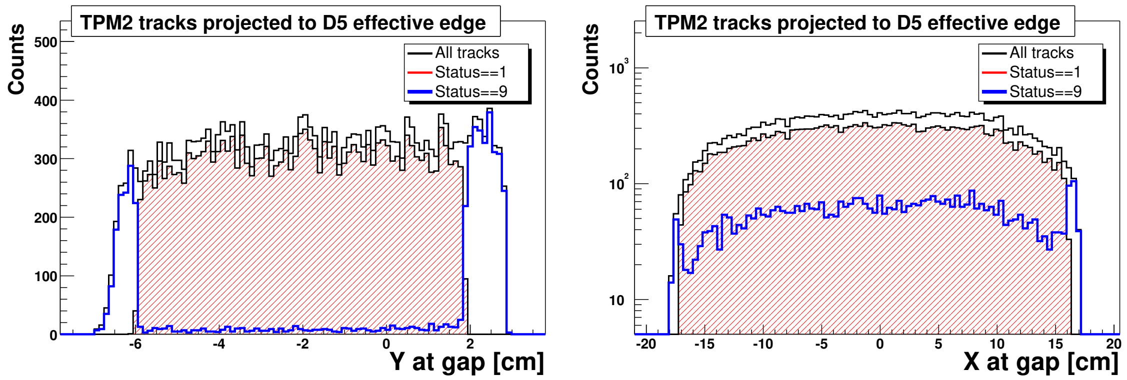

Figure 2: TPM2 track position at the D5 effective edge. Status 1 tracks are accepted and status 9 tracks are rejected by the magnet fiducial cut.

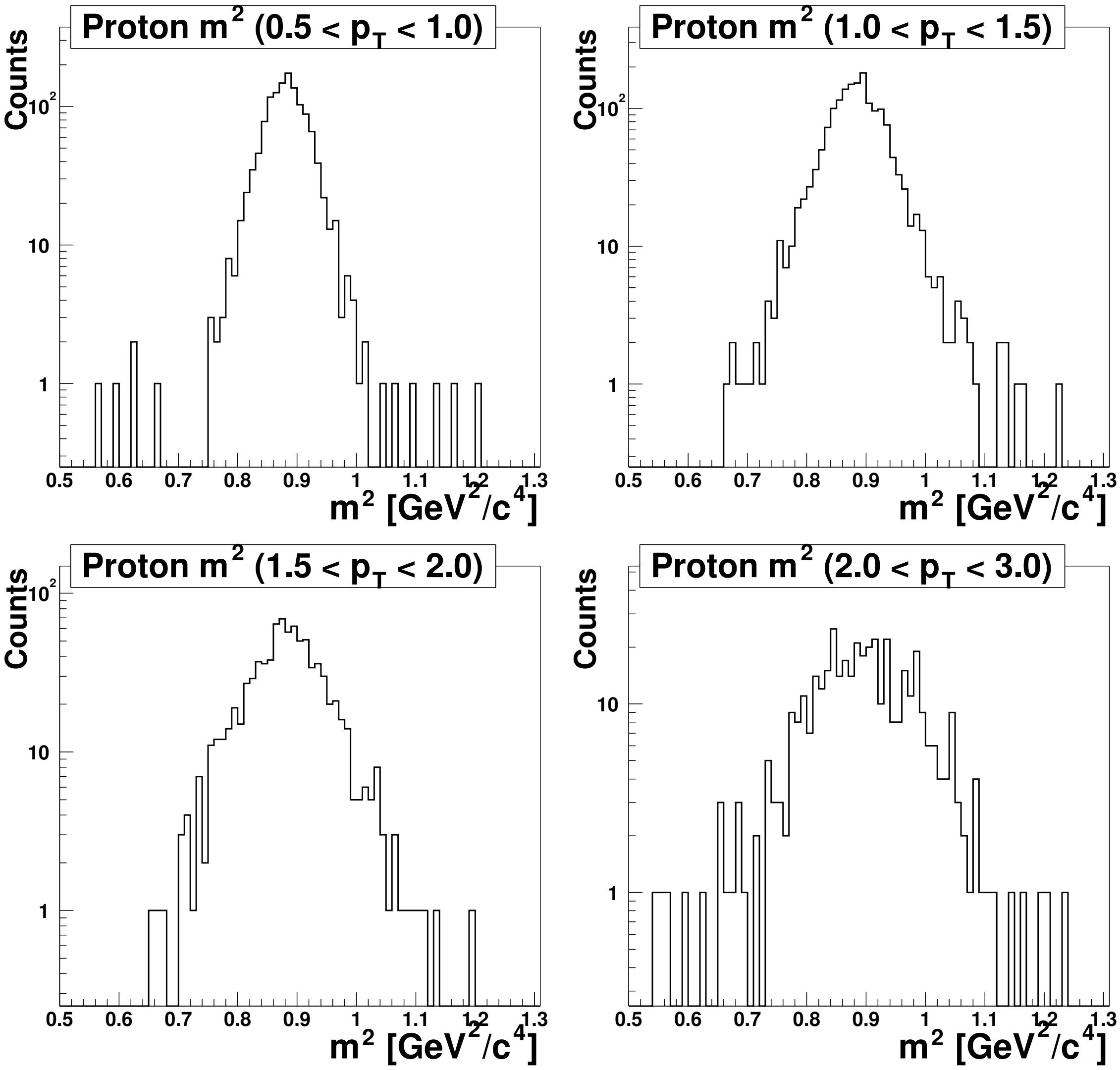

Figure 3: TOFW PID at 90 degrees. Each plot shows the protons selected by the m^2 cut in a small p_T interval.

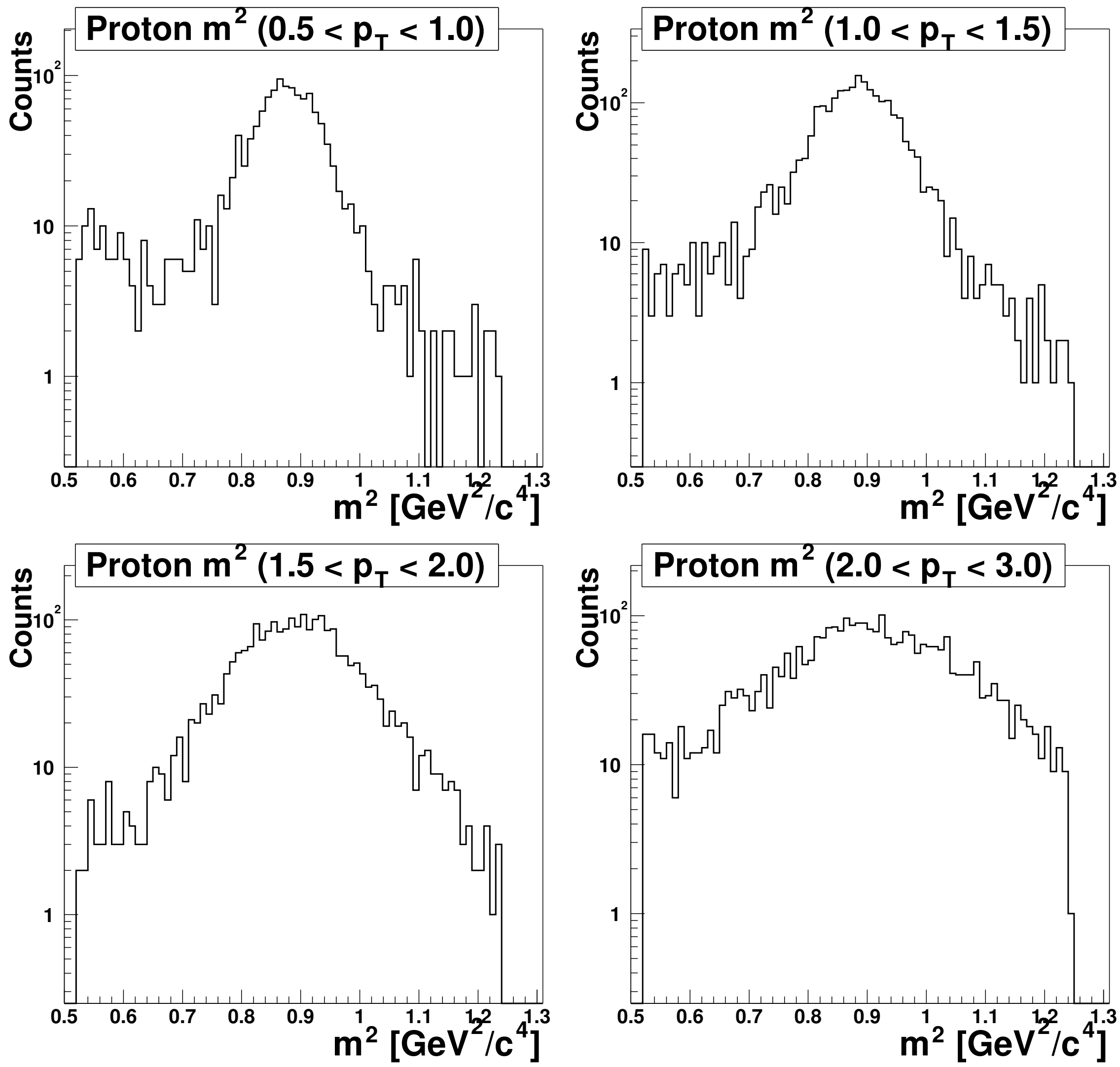

Figure 4: TOFW PID at 35 degrees. Each plot shows the protons selected by the m^2 cut in a small p_T interval. In the last figure the cut is 2.5 sigma.

Type	Cut	Explanation
GLOBAL	Abs(BBvtxZ) $<$ 15 cm	Acceptance
GLOBAL	BB Method = 1 or 2	BB Method 3 has bad resolution
GLOBAL	Centrality = 0-10 %	Centrality cut
TRACK	Status = 1	Fiducial and ghost cuts
TRACK	slat $>$ 25 and slat $<$ 103	Bad TOFW calibrations
TRACK	slat $\neq$ 31, 76, 92	Bad TOFW slats
TRACK	Δslat $\leq$ 1	Point to TOFW slat
TRACK	Δy slat $<$ 3 cm	Point to TOFW hit
TRACK	Abs(vtxY) $< 3\sigma_Y$	Point to vertex y
TRACK	Abs(vtxZ-BBvtxZ) $< 3\sigma_Y$	Point to vertex z
PID	Abs(p) $<$ 3.0 GeV	PID momentum cut
PID	$\Delta m^2 < 0.36$ GeV^2/c^4	proton cut

Table 1: Summary of cuts used in the MRS to select protons and anti–protons. GLOBAL means that the cut rejects events. TRACK means that it reject tracks. PID means that it is used to select protons.

The data is divided according to the BB vertex position. The reason for this is that the geometrical acceptance depends on where the interaction took place. In both the MRS and the FS, 5 cm bins have been used. In the MRS the output from the data selection is therefore proton $y - p_T$ distribution for each vertex range ((-15)–(-10), (-10)–(-5), (-5)–0, 0–5, 5–10, and 10–15). Figure 5 shows the proton distribution for one of those vertex bins (90 degree 350B) and a projection onto the p_T-axis of one rapidity bin. The next sections will focus on how to correct this for acceptance and efficiency and to combine different vertex bins and many other settings to get good statistics spectra.

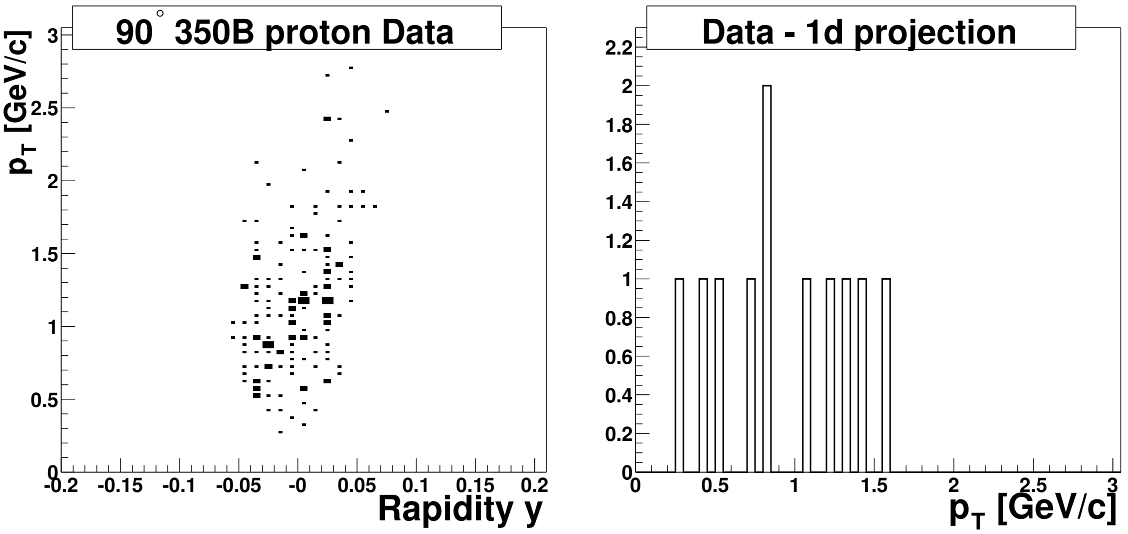

Figure 5: Protons selected in one (short) setting for one vertex bin.

2.2 MRS Efficiency

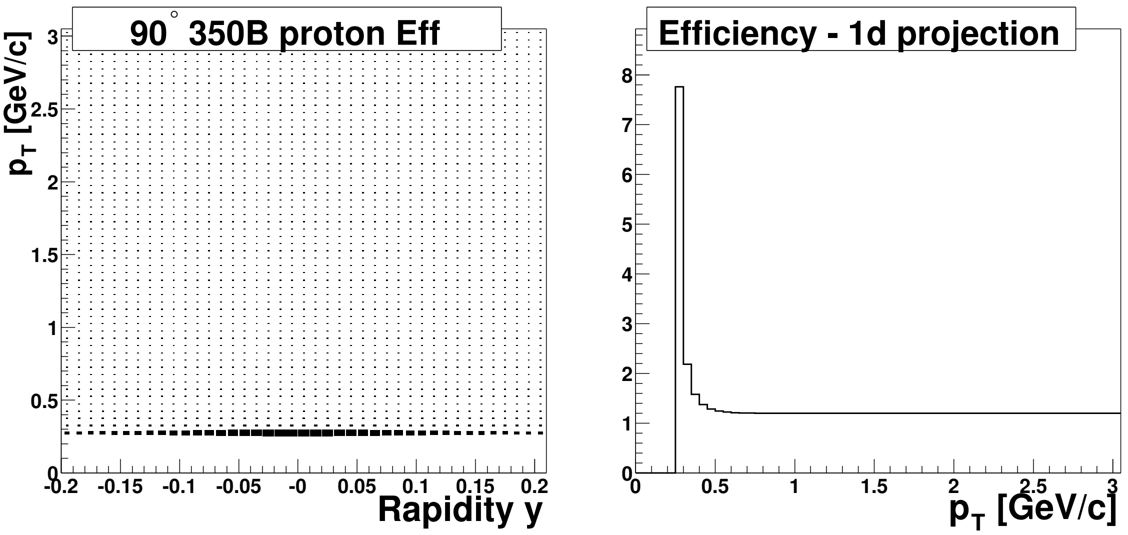

Figure 6: Proton efficiency correction. The correction has contributions from tracking efficiency, slat efficiency, multiple scattering, and absorption.

The data have to be corrected for tracking efficiencies, PID efficiency, multiple scattering and absorption. The background correction for protons knocked out from the beam pipe, experiment, air etc. have not been estimated yet.
The correction for tracking efficiencies was done in a quick way since I wait for the correction obtained with track embedding from Oslo. It was done analogous to Pawels method where you have a reference track and look for it. For the MRS, a TPM2 track was used as a base track requiring that it pointed to the vertex and hit the pointed slat. This is only possible for zero–field runs (since there is no way to learn the momentum from the TPM2 track). The method has been described in [1]. The efficiency has a weak dependece on angle and centrality (only trigger 6 was used) that has been ignored in the following and it is $\approx 92\%$. This is only the TPM1 efficiency but has been used for the total tracking AND matching efficiency.
The PID efficiency boils down to the slat efficiency in this case and that has been estimated by comparing how often a pointed slat had a signal. The slat dependece is almost flat and an overall efficiency of $\approx 91\%$ was found.
The correction for multiple scattering and absorption was done by Eun–Joo Kim [2]. The corrections are similar for the two angles (90 degrees and 40 degrees) where they have been computed and only depend on the momentum.
In Figure 6 the full 2 dimensional efficiency correction function for the 90 degrees setting is shown together with a projection of a single rapidity bin. At high momentum only the slat and tracking efficiencies have to be taken into account while at low momentum the absorption and multiple scattering dominates.

2.3 FS Selection

The FS PID selection depends on the momentum of the particles. Only the RICH ($p > 11$ GeV/c) and H1 ($p < 5$ GeV/c) has been used for this analysis. The track selection is the same in both cases and will be desribed first. If there is a track in the BFS it has already been checked that the D3 and D4 swim status is good at the dst level so it is only the FFS that needs to be checked.
Before the selection, the projection of all tracks to a perpendicular plane positioned at the interaction points is fitted with gaussians to get the horizontal and vertical resolution (both are typically of the order 0.6–0.8 cm) and the offsets. The track selection cuts applied is first a check to see if the momentum has the right sign ($-$ for A polarity settings and $+$ in B). Then the track projection back to the interaction point is applied a 2.5 σ elliptical cut and the swim status of the D1 and D2 magnet is required to be good.
The PID selection is currently done with a mass squared cut in the FFS in a narrow momentum range where protons are seperated from pions and kaons ($p < 5$ GeV/c) and with the RICH in the FS. The H1 selection is similar to the TOFW selection.
The RICH PID is shown in Figure 7. The threshold for identifying protons using the ring radius is high ($p \geq 16$ GeV/c) so it is important to use the RICH as veto for pions and kaons to get to low p_T and have a better coverage of the yield. The way protons are currently selected is that everything is a proton that is in the proton band AND all particles with momentum above 11 GeV/c that does not match up with a ring. In the bottom plot (Figure 7) it is seen that there is some background at high momentum in the veto sample (blue), but more importantly there seem to be a smooth cross–over between the two methods.
Figure 8 shows the H2 mass spectrum for the pions, kaons, and protons identified by the RICH. The protons are located at roughly the right mass and the shape seems to be gaussian. If the spectra was heavily contaminated (fx. due to a low RICH efficiency) then the distribution should have non–symmetric tails in the low mass region where the pions and kaons are. Djamel and I have done some tests where we have included cuts in H2 to see if there was any sigals of a large contamination. We concluded from these tests that the method is sound.
One test I did was to cut at the peak in the H2 mass for the protons and make a low ($h2mass^2 < cut$) and a high sample ($h2mass^2 > cut$) and for both samples require that the rich PID was a protons. The ratio of the spectra created this way to the original is shown in Figure 9. The flat p_T ratio and the level suggests to me that the contamination must be low ($< 5\%$) and should not affect the slope of the spectra.
Flemming has looked at the PID efficiency in much better detail than what was done here [6] and he finds that there is $\approx 3 - 5\%$ contamination in the anti–proton sample.

2.4 FS Efficiency

The FS tracking efficiency has been studied by Pawel Staszel in great detail [3, 4]. The corrections are stored in a file as 3–dimensional histograms. The coordinate axis are local coordinates of each tracking detector horizontal (x) position, horizontal slope, and centrality. There is no explicit momentum dependence.
The H1 correction was done similar to the TOFW correction (section 2.2) and the RICH efficiency correction was calculated as a function of the velocity β by Pawel by selecting tracks identified by H1 and H2 as pions and looking to see if they were identified in the RICH as pions. Average efficiency files should go here.

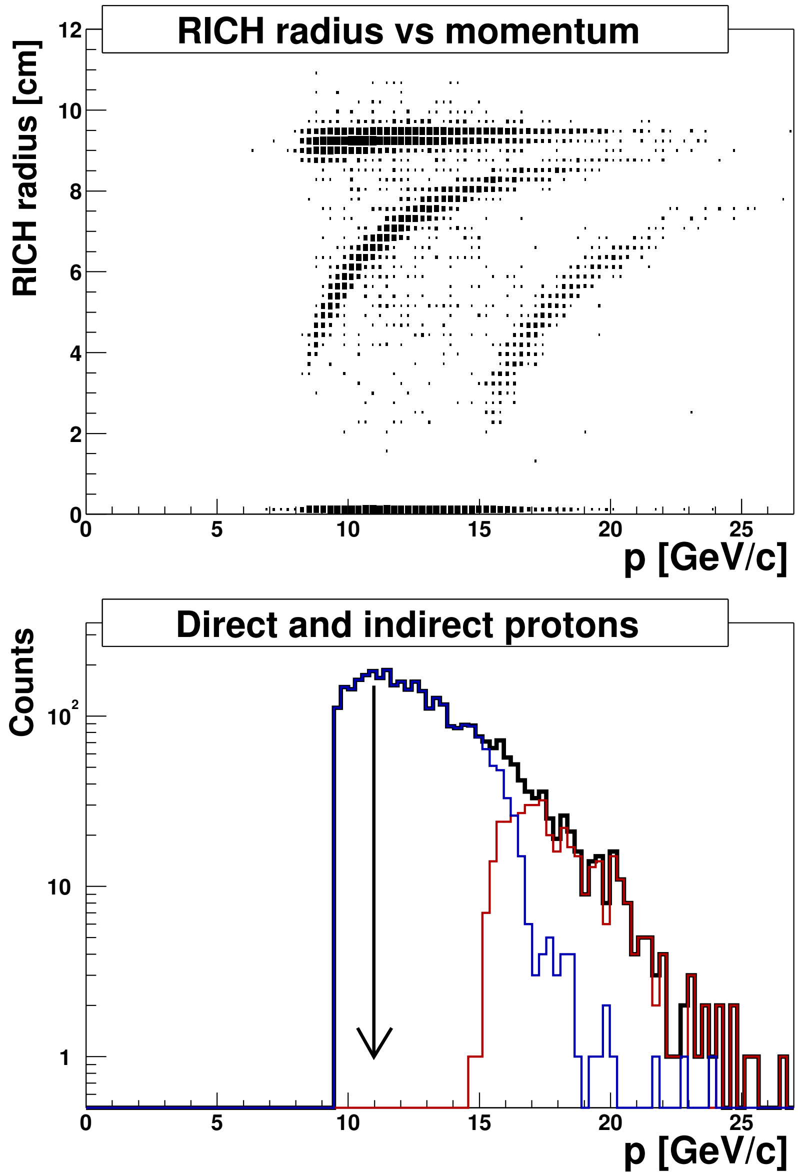

Figure 7: The RICH PID. The bands in the top plot corresponds to pions, kaons, and protons. Below is shown the momentum distibution for protons (black) and the component from direct selection (red) and where protons have been selected by vetoing pions and kaons (blue). The arrow indicates the momentum cut applied to the selection ($p > 11$ GeV).

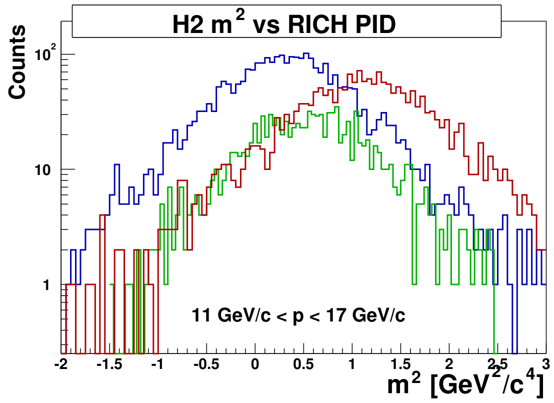

Figure 8: The H2 mass squared spectraum for pions (blue), kaons (green), and protons (red) identified by the RICH in the momentum interval ($11 < p < 17$) where the veto method dominates.

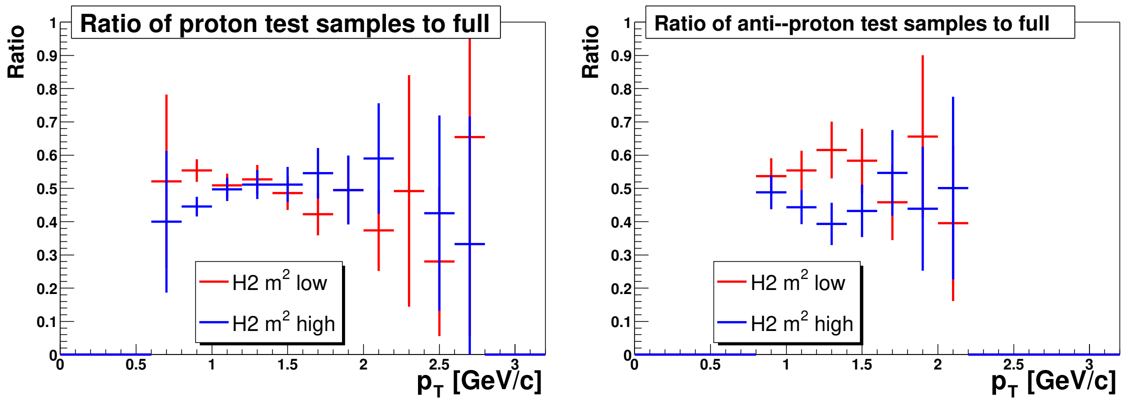

Figure 9: The plots show the ratio of the test samples made with H2 m^2 cuts discussed in the text to the spectra with RICH PID only.

The correction for multiple scattering and absorption was done by Eun–Joo Kim [5]. The corrections have been done at two angles, 12 degree and 3 degree. Here the 12 degrees correction was used for both the 8 and 12 degrees, and the 3 degree correction was used for 3 and 4 degrees.
HOW IS IT APPLIED!!!!!!!!!!!!

3 Acceptance

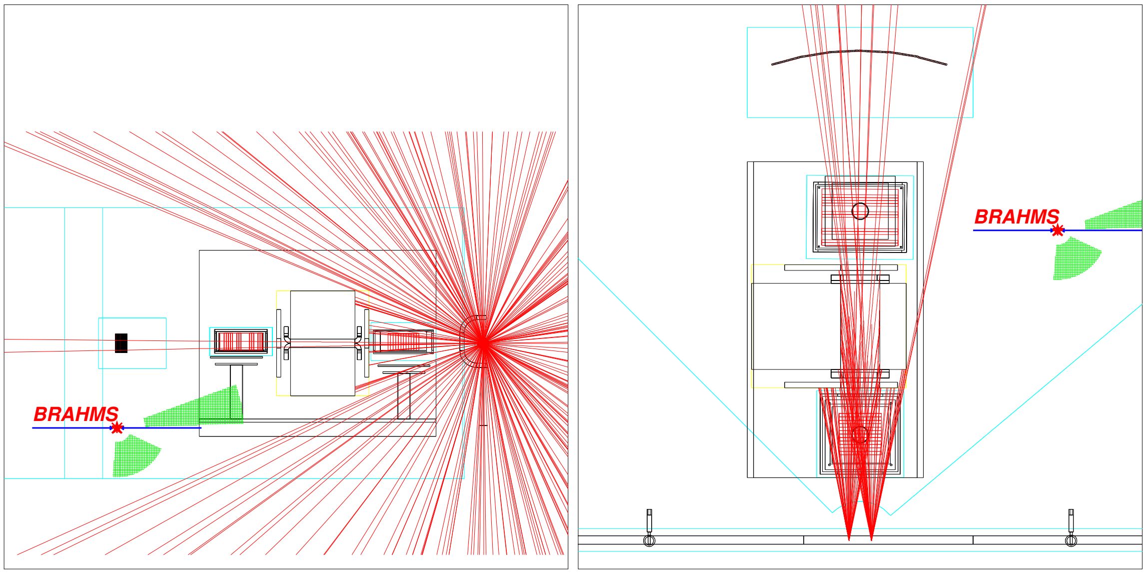

Figure 10: The plots illustrates some of the features the geometrical acceptance correction has to correct for.

Figure 10 illustrates that we have to correct for a very small solid angle coverage and that this correction depends on the IP. The acceptance is purely geometrical and is calculated from Monte Carlo simulation. A flat distribution of single particles is generated in a solid angle covering the magnet gab. In the simulation they are propagated through the detector setup and it can afterwards be determined if a particle was detected. The acceptance for a single vertex interval can then be calculated as :

$$ACC(y, p_T) = \frac{ACCEPTED(y, p_T)}{THROWN(y, p_T)} \times \frac{\Delta\phi}{2\pi} \quad (1)$$

To keep most information about the correction we keep the dependence on rapidity, y. The last factor ($\Delta\phi$) reflects that we don't throw particles in the full 2π because that would be a waste of CPU, see Figure 10. Figure 11 shows the histograms used to build an acceptance map.
In the simulation most physics is turned off so the simulation will be identical for pions, kaons, and protons i.e., a $p - \theta$ description of the geometrical acceptance would be identical. However, when rapidity y is used to characterise the phase space, a map is needed for each particle species. In the simulation only pions is generated, kaon and proton maps are created

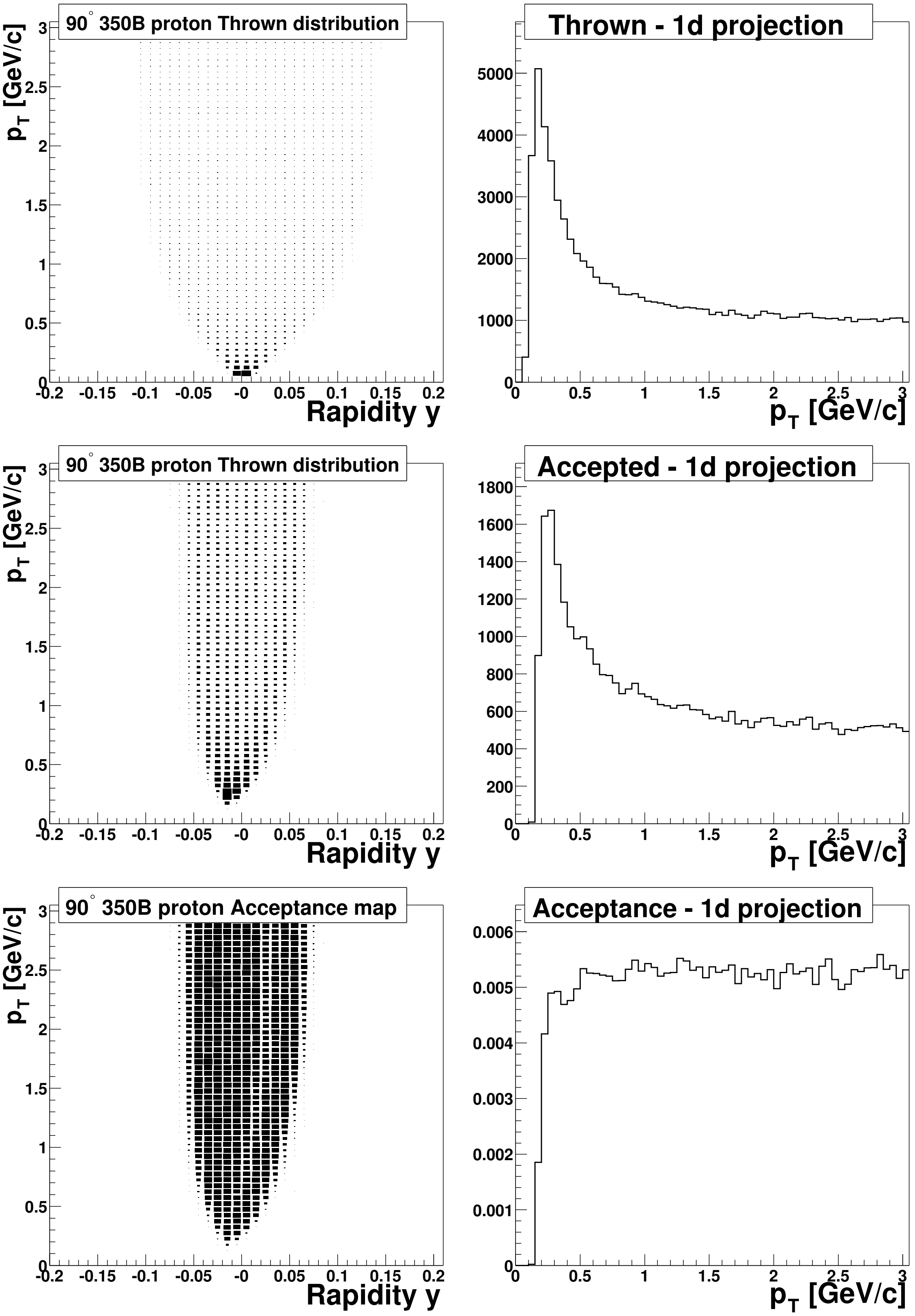

Figure 11: The construction of the Acceptance map. The top row shows the distribution of thrown protons. The middle row shows the protons accepted. The bottom row shows the final acceptance map.

afterwards by recalculating the rapidity using the respective masses instead of the pion mass. This means that when we want to compare different particle species (fx. kaons and pions) at the same rapidity we might need different settings.
Maps generated for positive particles can be used for negative particles in settings where the polarity is reversed, and vice–versa.

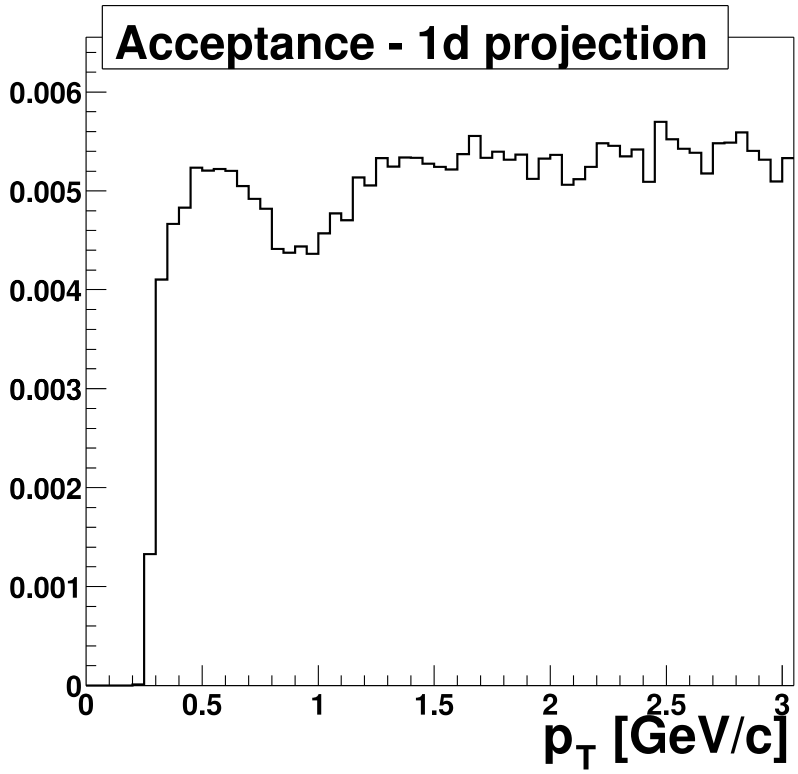

Figure 12: The plots shows the effect of a missing slat.

Before tracks are accepted there are some steps that are similar to the treatment of the real data. First the hits in the TPC's are grouped into local tracks and then the tracks are matched, the swim status is calculated and tracks that come closer than 1cm to the magnet are rejected. Finally it there is a slat cut like for the MRS (see Table 1). In figure 12 the effect of a missing slat is shown.

4 Spectra and fits

For each vertex range we have the number of events and three 2-dimensional histograms, data, corrections and acceptance.
The correction histogram is first divided by the acceptance histogram and normalised to the number of events and the bin sizes. This is done so that Equation 3 is fulfilled i.e., the spectra is calculated in a very simple way as the product of the measured counts and the correction. The 3 histograms listed below are the base objects of the spectra analysis. For the analysis I use the class **SpectraObject** that can be found in `brahms_app/pc_app/brag/acceptance`.

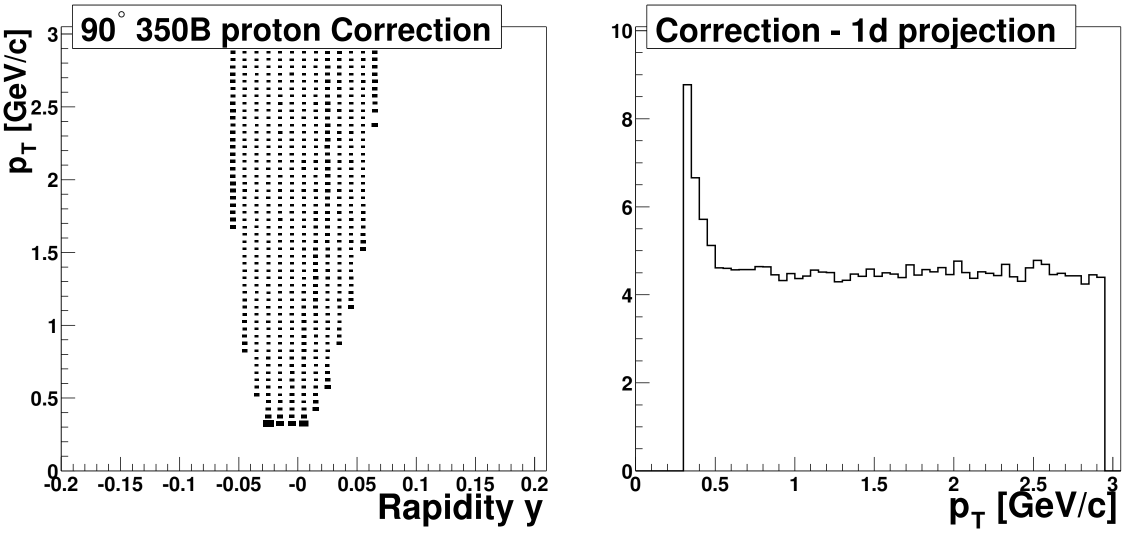

Figure 13: Proton correction function. The correction function takes into account the acceptance, the efficiency, and the normalization due to bin sizes and events. The correction function have been truncated at $p < 0.3$ where the efficiency correction is very large.

- Data. The selected particles.
- Acceptance. Geometrical acceptance including non-instrumented pads and slats normalised to full 2π azimuthal coverage.
- Correction. Efficiences, geometry, absorption etc. normalised to the number of events AND the bin size.

The acceptance is still important since we use that to remove the edges of the acceptance map. This is both where things have the strongest vertex dependence, and where we are most likely to have some problems with background from fx. the magnet. The average acceptance for a cell away from the edges follows the approximate scaling rule $avg(\theta) \sim avg(\theta = 90^\circ)/\sin(\theta)$ ($\theta \gg 0^\circ$). So at forward rapidities (lower θ) the inhomogenities in the map becomes more significant i.e. the level changes over the map.
The acceptance map at this stage contains no PID requirement. Because of the TOFW resolution, pions, kaons, and protons has a momentum threshold above which we cannot identify them. It is important to remove the corresponding cells from all the histograms, especially when we go away from midrapidity where the momentum cut is not almost constant in p_T. At low momentum the decay, absorption, and multiple scattering corrections are very high ($\gg 1$) and here a cut is used to remove cells where the corrections are large (> 2). The momentum cuts are shown in table 2. All protons with momentum below 0.3 GeV are absorbed and then the correction becomes very small rapidly.
For a cell in $y - p_T$ the momentum can be calculated when we know the mass m as :

$$p = \sqrt{(m_T * \cosh y)^2 - m^2} \tag{2}$$

where y and p_T are taken at the center of the cell.

Particle	Low cut	High cut
pi	0.3	1.95
K	0.4	1.95
p	0.5	2.95

Table 2: The cuts applied to the MRS histograms to limit the size of the corrections applied (low cut) and to reflect the PID range.

The acceptance defines where we keep the cells in the data and correction histogram. The 2d-spectra, $SPECTRA(y, p_T)$ is then obtained by multipliing the data histogram with the correction histogram (The multiplication is done cell by cell) :

$$SPECTRA(y, p_T) = DATA(y, p_T) \times CORR_{FINAL}(y, p_T) \tag{3}$$

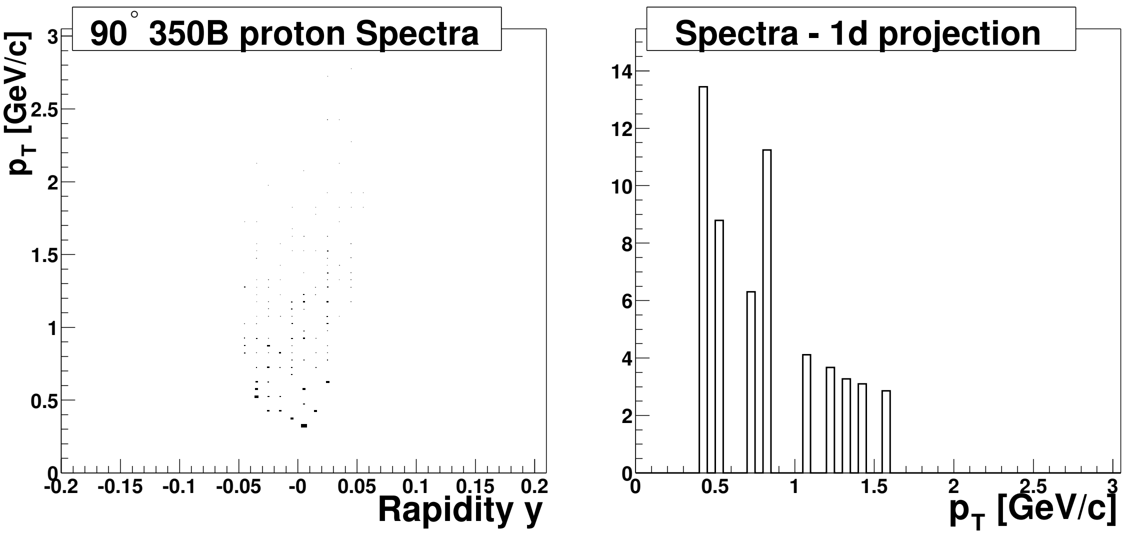

Figure 14: Proton spectra for one setting and one vertex bin. By combining many settings and vertex bins we can make a better spectra.

If the result for a cell is zero there can be 2 reasons. The simple reason is that the correction factor $CORR(y, p_T)$ is zero. This means that we are in a region where we we don't expect or trust counts. The second reason is that the data count $DATA(y, p_T)$ is zero. We cannot ignore this if $CORR(y, p_T) > 0$ since it means that we had a valid measurement with 0 counts. What we have to realise is that the inverse of the correction is the weight of the bin (from now on called $WEIGHT(y, p_T)$). The weight is proportional to the number of events AND the efficiency for detecting a proton, so in some sence it can be thought of as an effective number of events, when the number of counts pr event in each cell is low. The weight can be used to compare different settings and runs. To add many settings (vertex, runs, angle, field) the procedure is to add the correction histograms where each cell has the content inverted and finally invert the sum (like parallel resistors). Then you sum the DATA histograms and calculates the spectra by Equation 3. This way the 0's are treated correctly.

To make 1-dimensional projections the same procedure is used. For each p_T bin the CORR and DATA histograms are summed up for the rapidity bins used and the ratio is the best eatimate. For the 1–dimensional projections the final histogram has each bin divided by the transverse momentum to get the full normalisation. In the appendix of this note, I have tried to make a mathematical argument for why you have to sum the spectra in this way.

5 Temperature and Yields

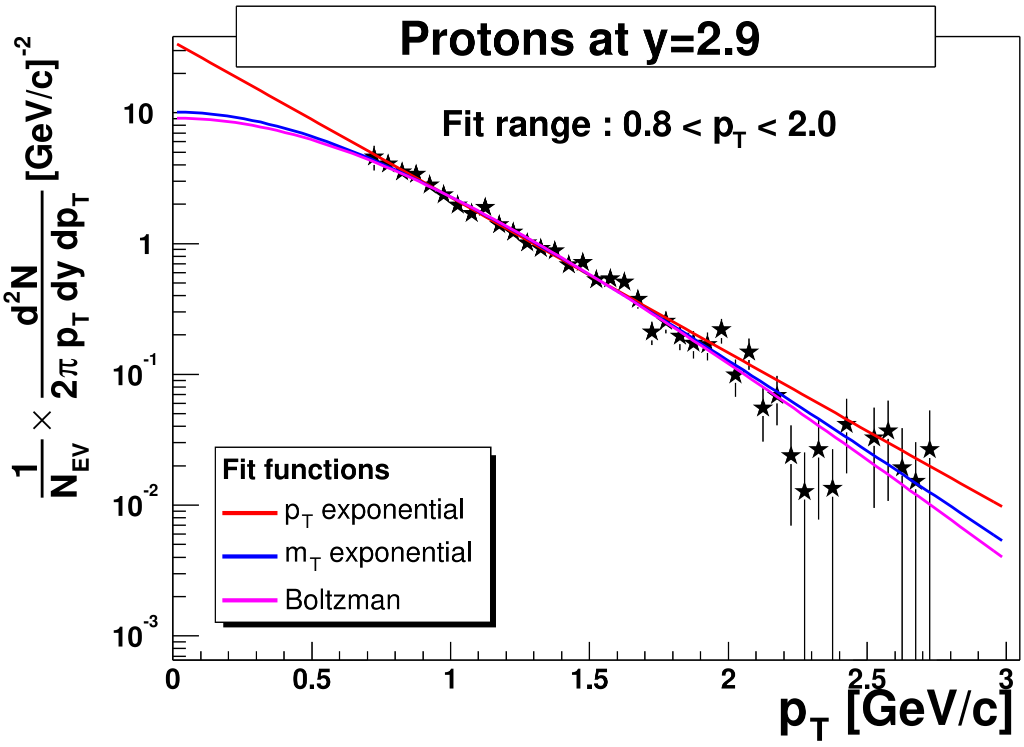

Figure 15: Proton spectra at rapidity $y = 2.9$ fitted with 2 different fit–functions. The functions are hard to distinguish in the measured data–range, but gives very diffrent yields when extrapolated to low p_T.

To get the total proton yields at a given rapidity we have to project the 2d–distributions and extrapolate the measured yield under the curve to where we have no data. To extrapolate the yield I fit the distribution with a m_T exponential which has the following parametrisation in p_T coordinates :
Figure 15 illustrates the different extrapolation of fitfunctions that all fits the observed shown data well. I have used m_T exponential becuase it fits the data well at mid–rapidity AND forward rapidity and because it fits pions, kaons, and protons reasonably where the boltzman only works well for protons.

$$\frac{1}{N_{ev}}\frac{d^2N}{2\pi m_T dy dp_T} = \frac{1}{2\pi}\frac{dN}{dy}\frac{1}{T(T+m_p)}\exp\left(\frac{m_p}{T}\right)\exp\left(-\frac{\sqrt{p_T^2+m_p^2}}{T}\right) \quad (4)$$

6 Results

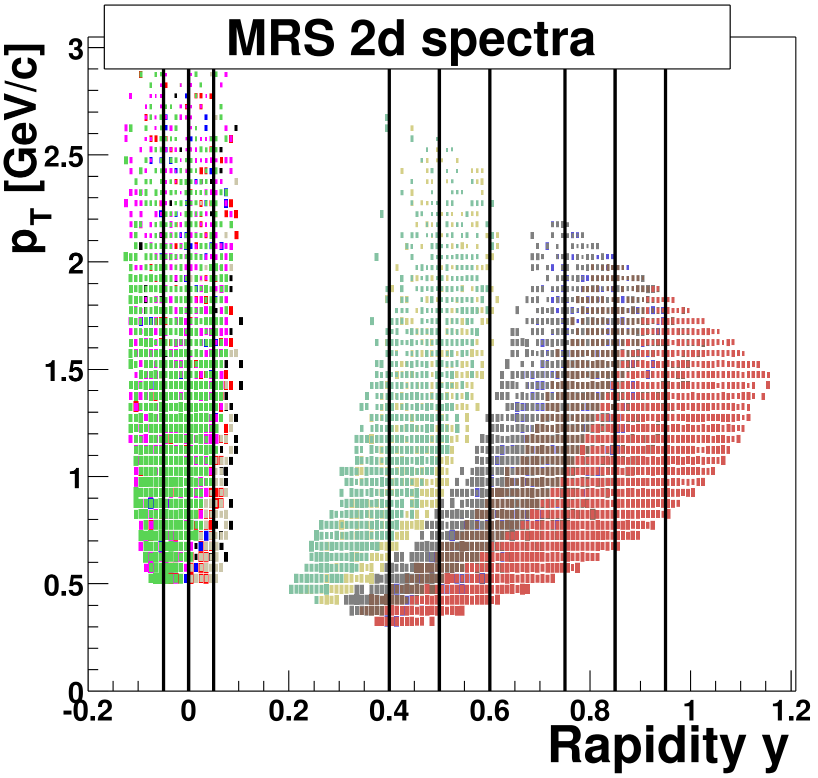

Figure 16: The phase–space (y, p_T) covered by the MRS with the settings used here. The black lines illustrates where the projections have been done.

Figure 16 and Figure 17 shows the coverage of the data used in this analysis. It also shows where the cuts in rapidity have been made. In Figure 18, 19, and 20 all the p_T–spectra are shown for protons and anti–protons. All the fits are done using Equation 4. I have tried to use the full data-range for the fits and always have the same range for protons and anti–protons. Sometimes I have ignored a few bins in the beginning if they looked very low. All the fits are χ^2 fits because I had some problems with maximum–likelihood fits in ROOT.
It is clear that there are some issuses that has to be solved in later iterations of the results. In my opinion there are 3 big problems with the results :

- $y = 0$ problem. Why are the 90 degree points much higher (especially the p–bar) than the other MRS points.

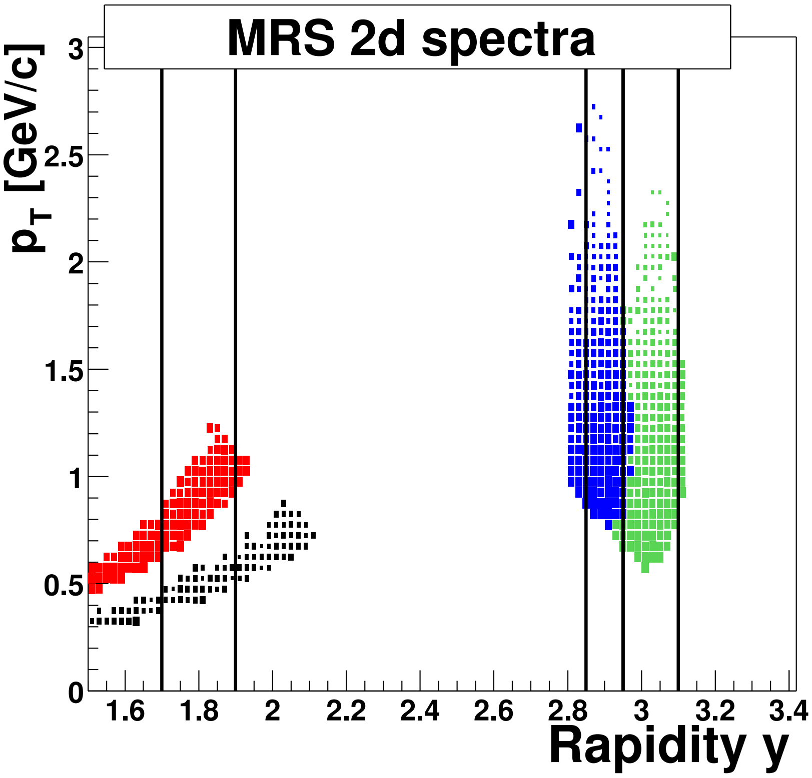

Figure 17: The phase–space (y, p_T) covered by the FS with the settings used here. The black lines illustrates where the projections have been done.

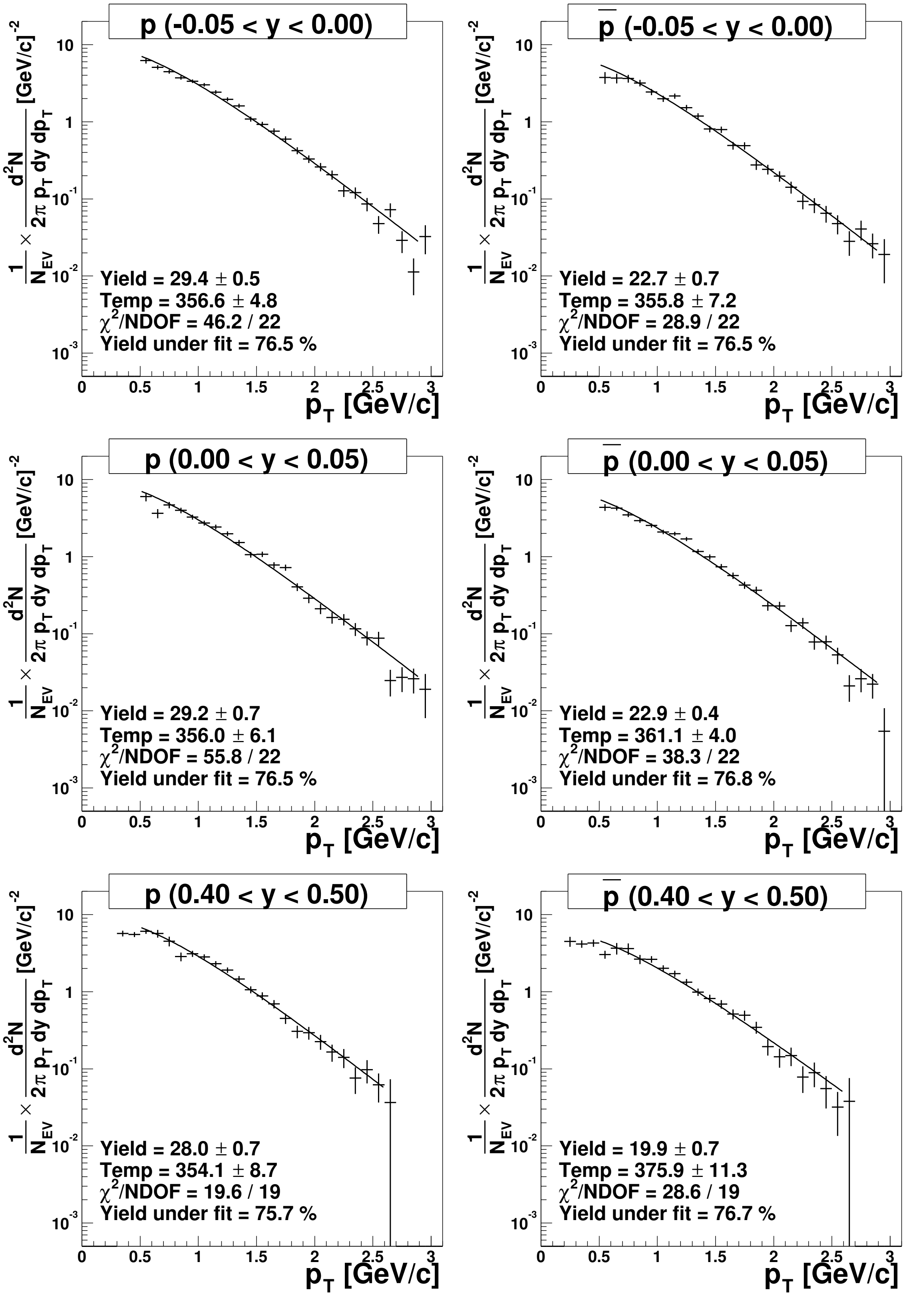

Figure 18: Spectra.

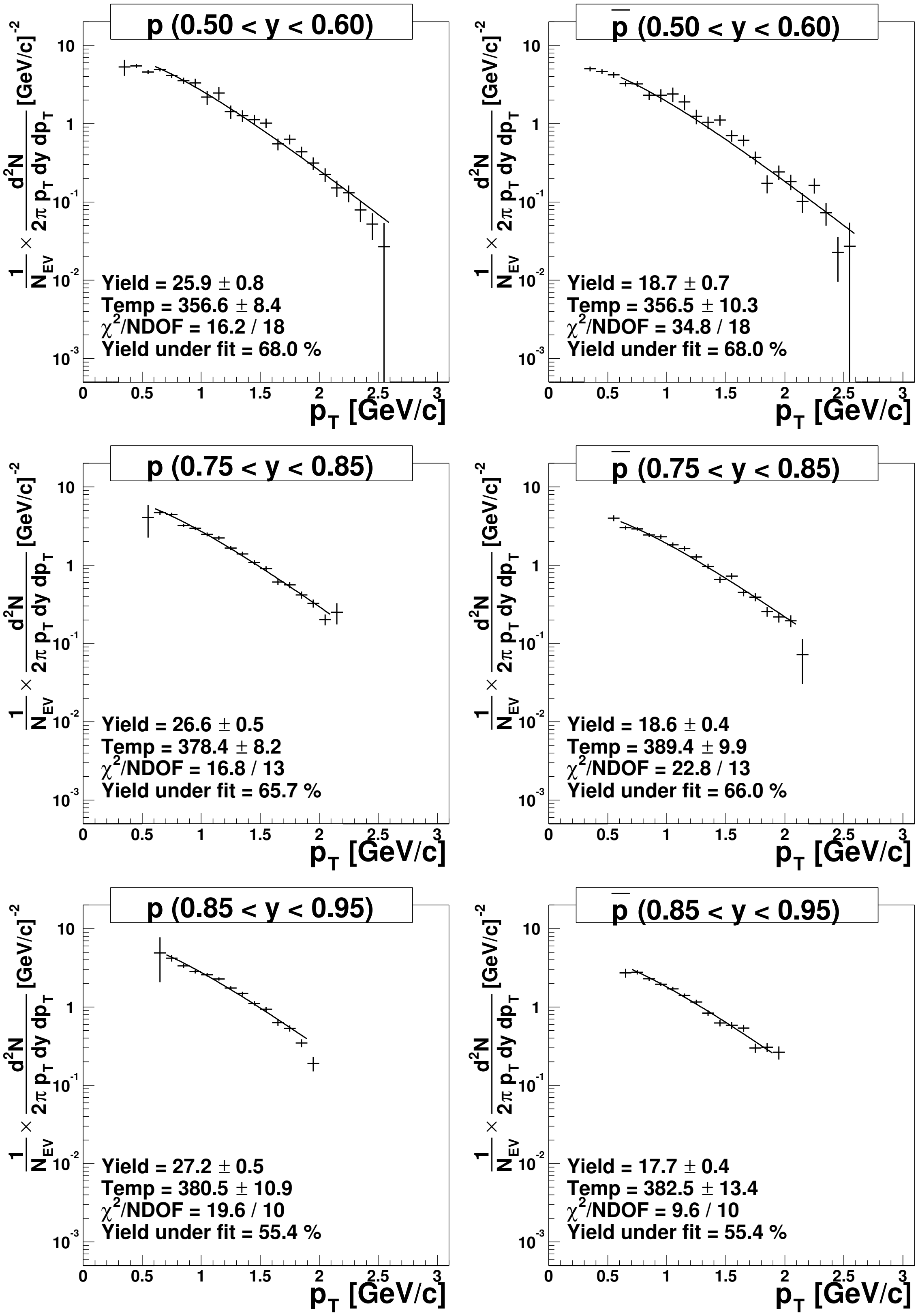

Figure 19: Spectra.

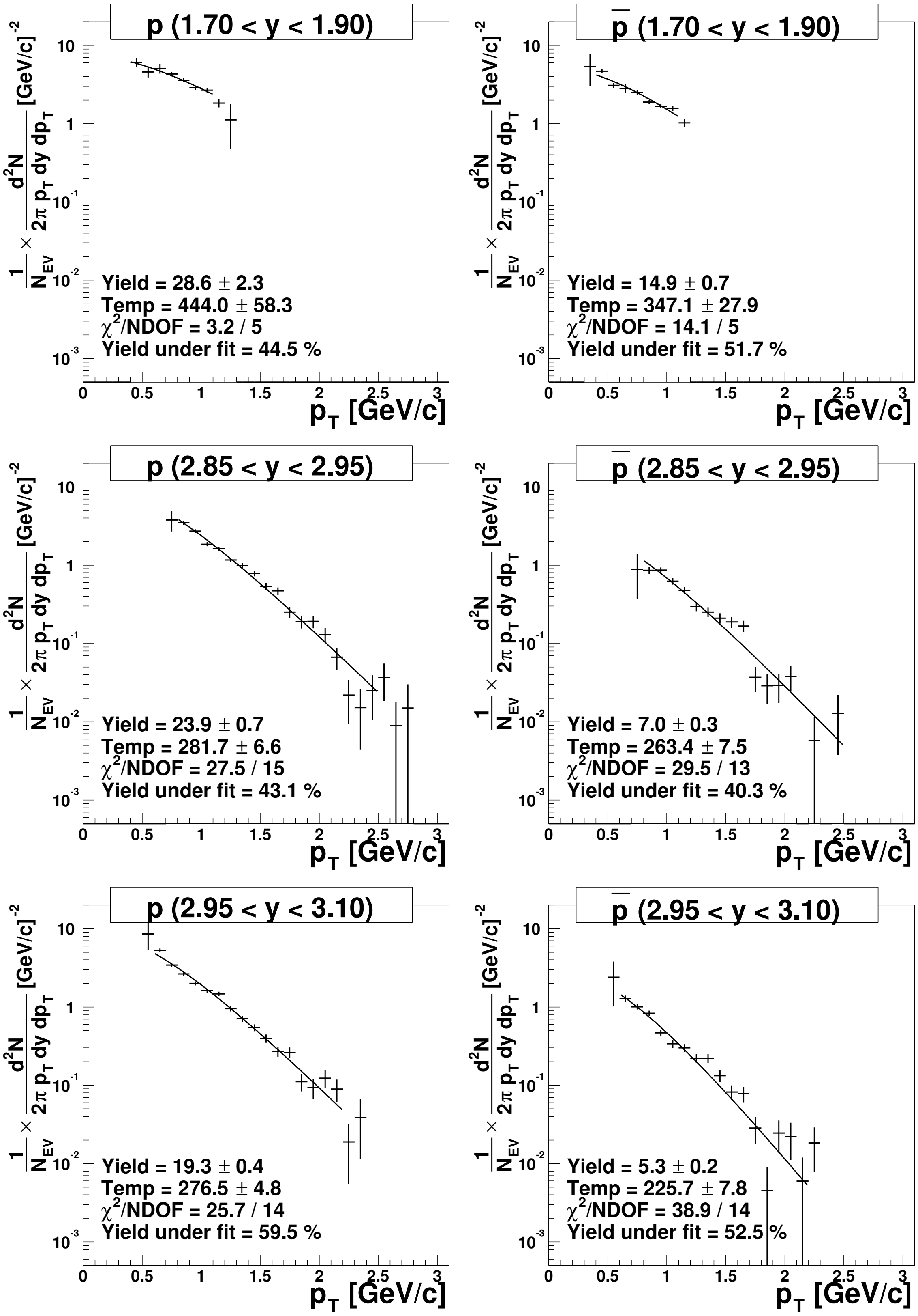

Figure 20: Spectra.

- $y = 2$ problem. We need better coverage and another data point. The quality of this point is not so good because the acceptance is very small and the H1 proton selection is not as easy as the TOFW.
- $y = 3$ problem. Why is there a 20% difference between 3 degrees and 4 degrees high field data.

These problems will not be solved the next month which is dedicated to writing, but after that I will look at the data again and try to finalize the data.

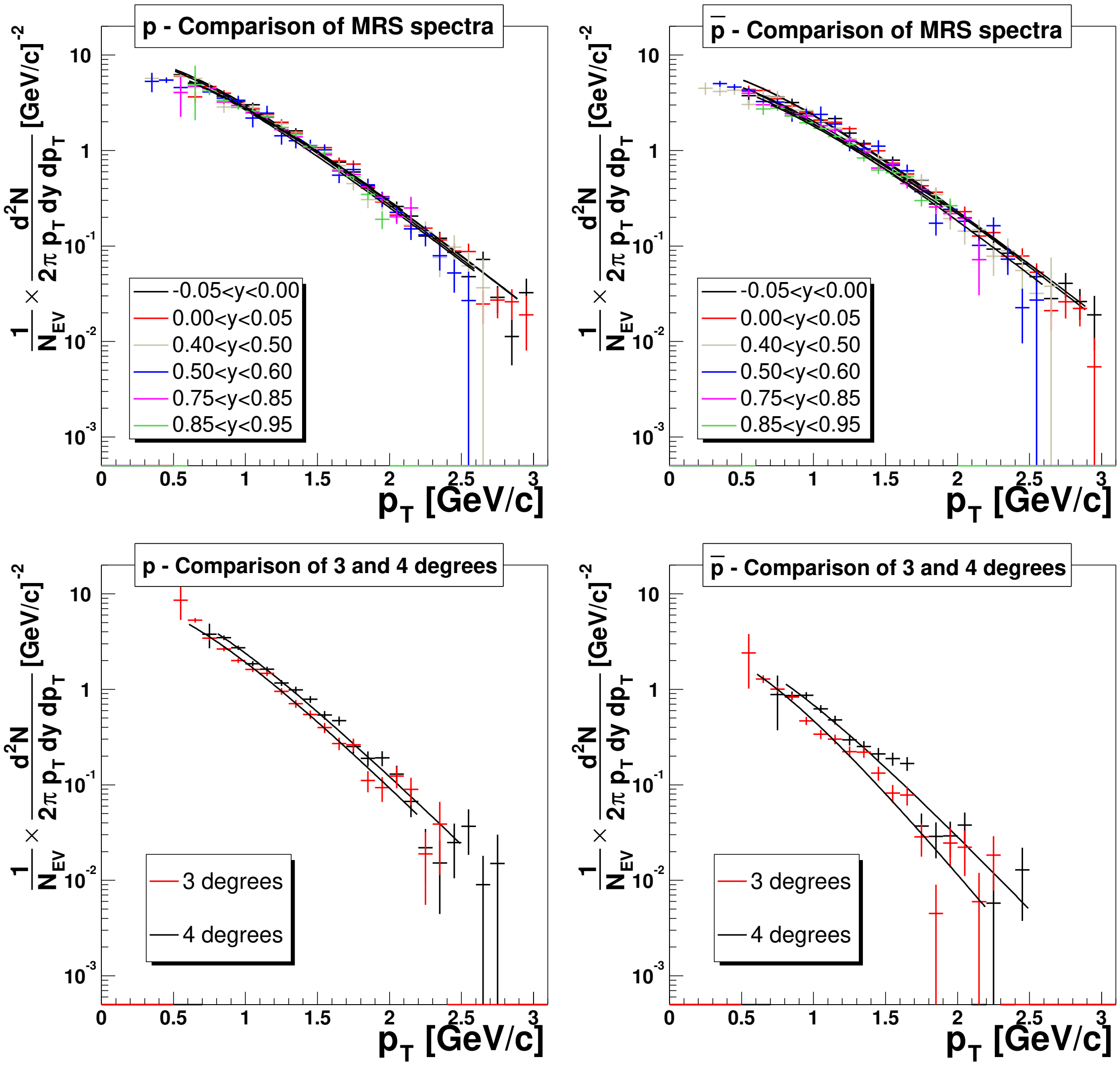

Figure 21: Comparison between proton (anti–proton) spectra from MRS (top) and FS (bottom). The fits on the plots I could not figure out how to avoid drawing in ROOT.

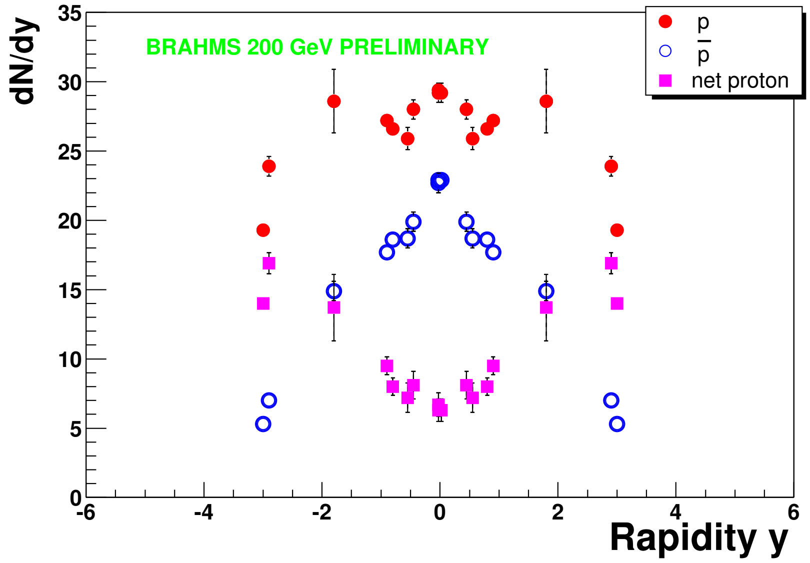

Figure 22: Integrated yields dN/dy as a function of rapidity for protons, anti–protons, and net–protons. The data are no corrected for feed–down of hyperons. Error bars are statistical only.

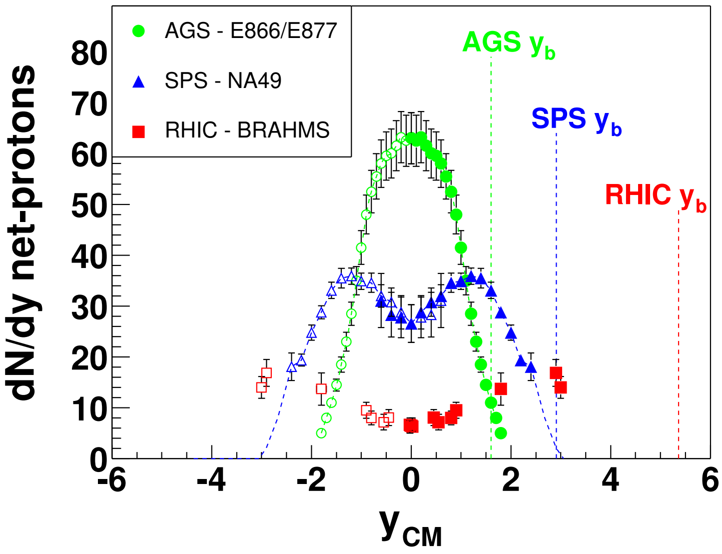

Figure 23: The energy systematics of the net–proton yields at AGS, SPS, and RHIC.

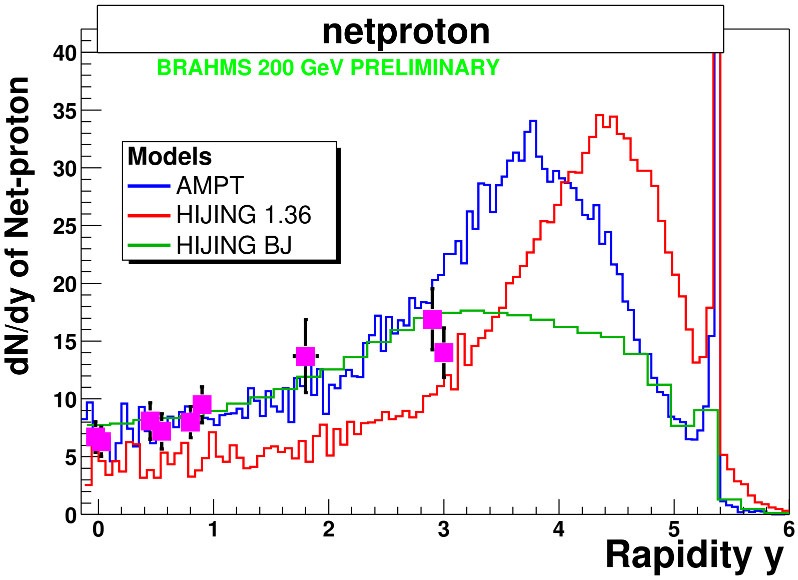

Figure 24: The net–proton distribution compared to the prediction of various models.

A Data used

Here I have included a list of the runs used. The runs not used is either because they are inherently bad or reduced badly (many runs in the 90 degrees 1000B sample have bad matching cuts) etc.

A.1 MRS

```
35 degrees B 700 :
5388, 5398, 5399, 5407, 5408, 5420, 5432, 5435, 5438, 5468, 5471,
5473, 5474, 5475, 5479

40 degrees A 1000 :
5544, 5548, 5549, 5553, 5556, 5557

40 degrees B 1000 :
5558, 5559, 5566, 5569, 5573, 5574, 5577

45 degrees A 700 :
5604, 5605, 5606, 5607

45 degrees B 700 :
5578, 5580, 5581, 5587, 5592, 5593, 5594

60 degrees A 700 :
5609, 5610, 5611, 5617
```

60 degrees B 700 :
5640, 5641, 5642, 5649, 5650, 5654

90 degrees A 350 :
5692, 5695

90 degrees B 350 :
5712, 5713, 5721

90 degrees A 700 (back) :
5763, 5765, 5766

90 degrees B 700 (back) :
5735, 5736, 5737

90 degrees B 1000 :
5895, 5896, 5903, 5904, 5908, 5910, 5914, 5915, 5916, 5924, 5925, 5937, 5938, 5939, 5945, 5946, 5947, 5948, 5952, 5953, 5954, 5956, 5957, 5958

A.2 FS

3 degrees A1692 :
5526, 5527, 5528, 5529, 5534, 5541,

3 degrees B1692 :
5557, 5559, 5566, 5569

4 degrees A1692 :
5479, 5482, 5483, 5485, 5494, 5495, 5508, 5509

4 degrees B1692 :
5468, 5471, 5473, 5474, 5475

8 degrees A427 :
5940, 5946, 5947, 5948

8 degrees B427 :
5952

12 degrees A427 :
5680, 5681, 5682, 5683, 5684, 5685, 5692

12 degrees B426 :
5662, 5664, 5665, 5677, 5678

B Summing of spectra

For some time I have thought about how to add the histogram cells in our $1/N * 1/p_T * d^2N/dydp_T$ distribution. The problem is when there are no counts. If there are counts, we have an error ($\sqrt{n}$) and can use the error as weight in a weighted average calculation.

B.1 The method

The information we have is measurements of $p_i = n_i/N_i * \varepsilon_i$:

- **p** Probability in one event for observing one particle in the cell ($1/N*1/p_T*d^2N/dydp_T$). This is what we want to find.
- $\mathbf{N_i}$ The number of events accepted in event sample.
- $\boldsymbol{\varepsilon_i}$ Overall acceptance, efficiency, $1/p_T$, etc.
- $\mathbf{n_i}$ The actual number of particles in the cell.

We want to find the best estimate for p and the error, $\hat{p}$ and $\sigma_{\hat{p}}$. The cell count n_i is Poisson distributed :

$$P(n_i) = \frac{\mu_i^{n_i}}{n_i!} \exp(-\mu_i) \tag{5}$$

where $\mu_i = N_i * \varepsilon_i * p$.
In the spirit of the maximum likelihood method we can construct the likelihood function :

$$L(p) = \prod_i \frac{\mu_i^{n_i}}{n_i!} \exp(-\mu_i) \tag{6}$$

Taking the logarithm :

$$\begin{aligned} \log L(p) &= \sum_i n_i \log \mu_i - \log n_i! - \mu_i \\ &= \sum_i n_i \log N_i\varepsilon_i + n_i \log p - \log n_i! - N_i\varepsilon_i p \end{aligned} \tag{7}$$

And differentiating with respect to p :

$$\begin{aligned} \frac{d \log L(p)}{dp} &= \sum_i \frac{n_i}{p} - N_i\varepsilon_i \quad \Rightarrow \\ \hat{p} &= \frac{\sum_i n_i}{\sum_i N_i\varepsilon_i} \end{aligned} \tag{8}$$

This expression has a simple interpretation. The nominator is the total number of measured particles and the denominator is the total number of tries scaled for efficiency etc.
The statistical error purely comes from the nominator and so the relative error on the calculated probability is the relative error on the nominator :

$$\sigma_{\hat{p}} = \frac{\hat{p}}{\sqrt{\sum_i n_i}} \tag{9}$$

B.2 A test simulation of the method

To test equation 8 and equation 9, I implemented a small root script (`brahms_app/pc_app/yields/sum/testTheory.C`) with a class that that takes the following arguments :

- **fNSamples** Number of "cells"
- **fEffLow** Minimum efficiency.
- **fEffHigh** Maximum efficiency.
- **fNLow** Minimum number of throws.
- **fNHigh** Maximum number of throws.
- **fProbability** Probability that the throw ends up in the cell.

The program then generates (call **Generate**) fNSamples distributions with random flat efficiency and a random flat number of throws and calculates the estimated probability and error.
One can now make many tests with the same parameters and compare the output to the input, see Figure 25. The only thing that is changed in the 3 simulation is the probability. The other parameters values are shown in Table 3.
In Figure 25 the histogram output from 3 tests is displayed. The top column shows the deviation from the input probability fitted with a Gaussian over the full range. The Gaussian fit is quite good, but we start to see small deviations at the edges when the probability goes down and the spread increases, because the deviation cannot go below 0. It is good to see that when we look at the calculated error (middle row) the mean agrees with the sigma. The width of the distribution illustrates the strong dependence on the number of cell counts. The bottom row shows the distribution of the deviation divided by the error. By doing that I hoped to get similar Gaussian distributions for the 3 cases with sigmas of 1.0. The first two cases are close to that, but the last is clearly not Gaussian. In case 3 you have a very low estimated number of counts ($\langle n \rangle = 10 * 1500 * 0.6 * 0.001 = 9$ where we are on the limit if errors are really Gaussian.

Params	**values**
fNSamples	10
fEffLow	0.2
fEffHigh	1.0
fNLow	1000
fNHigh	2000

Table 3: Parameters used for the 3 simulation.

B.3 Conclusion

I have examined how to add the cells in our yield histograms before we fit. It seems that as long as we stay to cells with counts greater than 10 we are in good shape, i.e, we have well defined Gaussian errors. When we get lower than that we probably have to use likelihood fits to treat the data correctly.

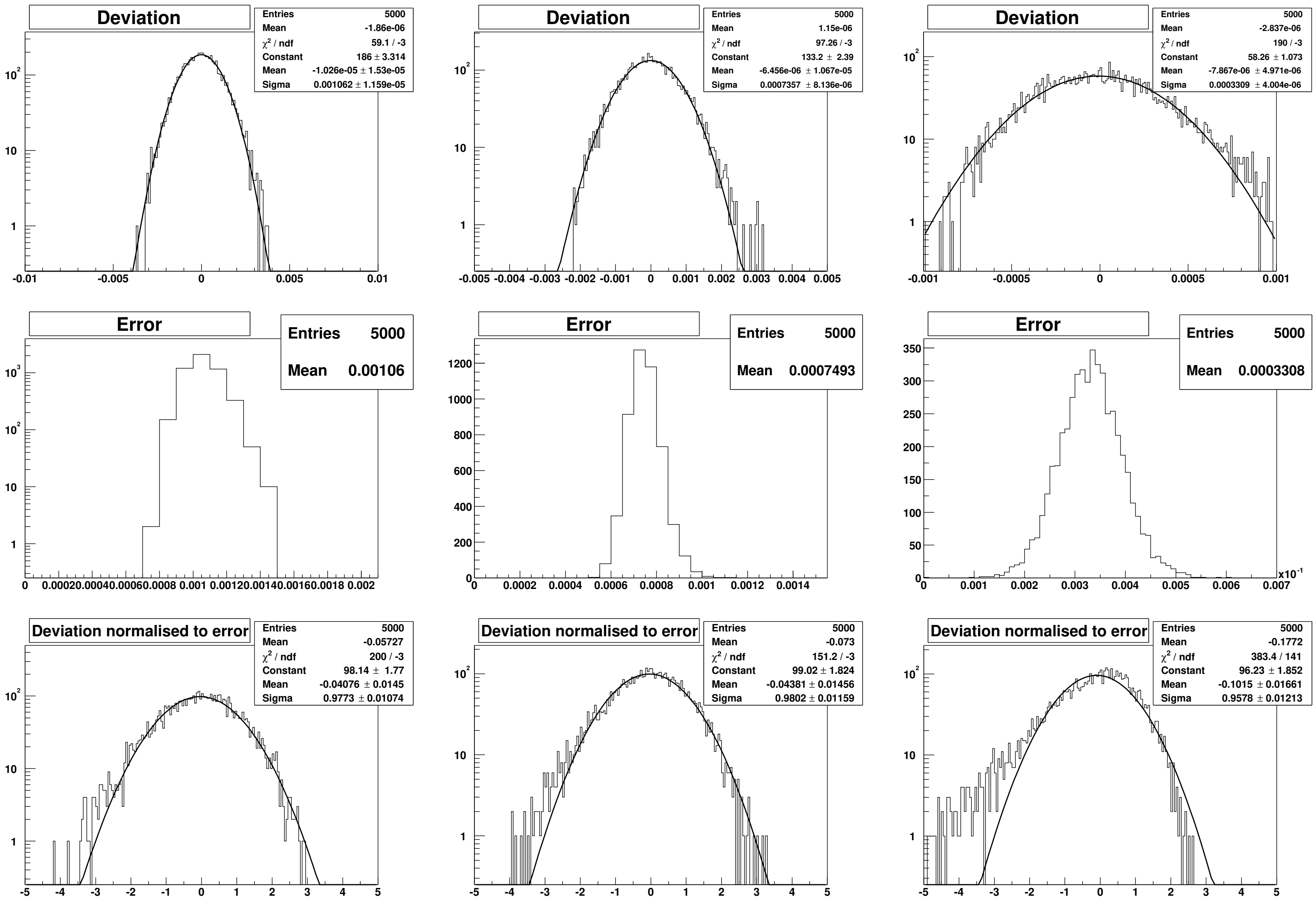

Figure 25: The output from the simulation for 3 different probabilities, p=0.10 (left column), p=0.05, p=0.01(right column).

References

[1] http://www.nbi.dk/~pchristi/BRAHMS/SPECTRA/tpm1eff.html

[2] http://pii3.brahms.bZnl.gov/~ejkim/brahms/mrs_cor.html

[3] P. Staszel, "Track Reconstruction Efficiency in FS Tracking Detectors" (BAN 38)

[4] http://www.nbi.dk/~staszel/fs/efficiency/index.html

[5] http://pii3.brahms.bnl.gov/~ejkim/brahms/fs_cor.html

[6] http://www4.rcf.bnl.gov/brahms/WWW/private/meetings/Dec2002/index.html